Actin-based biomechanical features of suspended normal and cancer cells

Seyed Mohammad Ali Haghparast[1], Takanori Kihara[1*], Yuji Shimizu[1], Shunsuke Yuba[2], Jun Miyake[1]

[1]Department of Mechanical Science and Bioengineering, Graduate School of Engineering Science, Osaka University, 1-3 Machikaneyama, Toyonaka, Osaka 560-8531, Japan

[2]Health Research Institute, National Institute of Advanced Industrial Science and Technology (AIST), 3-11-46 Nakoji, Amagasaki, Hyogo 661-0974, Japan

afshin@bpe.es.osaka-u.ac.jp (S.M.A.H.), takanori.kihara@gmail.com (T.K.), week127@yahoo.co.jp (Y.S.), yuba-sns@aist.go.jp (S.Y.), jun_miyake@bpe.es.osaka-u.ac.jp (J.M.)

*Corresponding author. Tel: +81-6-6850-6550, Fax: +81-6-6850-6557

E-mail address: takanori.kihara@gmail.com (T. Kihara)

Running title: Biomechanical features of suspended cells

Abstract

The mechanical features of individual cells have been regarded as unique indicators of their states, which could constantly change in accordance with cellular events and diseases. Particularly, cancer progression was characterized by the disruption and/or reorganization of actin filaments causing mechanical changes. Thus, mechanical characterization of cells could become an effective cytotechnological approach for early detection of cancer. To develop mechanical cytotechnology, it would be necessary to clarify the mechanical properties in various cell adhesion states. In this study, we investigated the surface mechanical behavior of cancer and normal cells in the adherent and suspended states using atomic force microscopy. Adherent normal stromal cells showed high surface stiffness due to developed actin cap structures on their apical surface, whereas cancer cells did not have developed filamentous actin structures, and their surface stiffness was low. Upon cell detachment from the substrate, filamentous actin structures of adherent normal stromal cells reorganized to the cortical region and their surface stiffness decreased consequently however, the stiffness of suspended normal cells remained higher than that of cancer cells. These suspended-state actin structures were similar, regardless of the cell type. Furthermore, the mechanical responses of the cancer and normal stromal cells to perturbation of the actin cytoskeleton were different, suggesting distinct regulatory mechanisms for actin cytoskeleton in cancer and normal cells in both adherent and suspended states. Therefore, cancer cells possess specific mechanical and actin cytoskeleton features different from normal stromal cells.

Keywords: Mechanical features, Atomic force microscopy, Suspended state, Cancer cell, Actin cytoskeleton, Mechanical cytotechnology

Introduction

Alterations in biological activities and transformation of cell states often entail a change in the mechanical behavior of cells. In particular, alterations in cell stiffness/elasticity have emerged as a marker for cellular phenotypic events and diseases. During optic-cup morphogenesis, a change in the stiffness of the retinal epithelium is important for the formation of neural retinal tissue (1). Malignant cancer cells exhibit lower stiffness than normal cells (2-4). Mechanical properties are largely attributable to the cytoskeleton components, especially actin microstructures which together are referred to as actin cytoskeleton (5-9). The above-mentioned stiffness alterations reflect the remodeling process of the actin and other cytoskeletal elements in the respective cellular events and disease states. Particularly, the actin cytoskeleton remodeling plays important role in the life cycle of a cancer cell. Actin depolymerization and disrupted stress fibers, marked by a shift from F-actin to G-actin, occur in the early stages of malignant transformation (10,11). Besides, abnormal F-actin distribution and dynamics occur in the later stages of cancer and correspond to tumor cell invasiveness and metastasis (12,13).Thus, sensitive and non-destructive estimation methods for the detection of actin cytoskeleton remodeling in cancer cells are powerful tools for early diagnosis of cancer. In this regard, stiffness and other mechanical properties are potent detectable targets in cancer cytotechnology.

There are several methods to detect cell stiffness and other mechanical properties including micropipette aspiration (14), optical stretcher (15), and atomic force microscopy (AFM) (16). These technologies measure the stiffness and mechanical properties of cells in the adherent or suspended states over a wide range of physiological conditions. Micropipette aspiration and optical traps are used with suspended cells, whereas AFM is generally used for substrate-adherent cells. Despite some drawbacks such as relatively slow measurement rate and low throughput, AFM has been incrementally used to directly measure the surface stiffness of substrate-adherent cancer cells in many studies due to its certain advantages (17-21). AFM can

investigate the mechanical properties of a cell surface with high sensitivity and spatial resolution under physiological cell culture conditions (22,23).

The most useful cytotechnology for detection of cancer cells, such as circulating tumor cells in the blood and biopsy for cancer, are applicable to the suspended cell state. Body fluid specimens may be the first and only pathologic specimen for clinical evaluation in metastatic cancer cases (24). Therefore, optical stretcher is one of the most useful methods to estimate whole cell stiffness in the suspended state (25), and the stiffness difference between suspended cancer and normal cells has been reported using this technique (3). Although structural differences in the actin cytoskeleton of cancer and normal cells are well understood in the adherent state (17,20), those of suspended state are unclear. Particularly, measuring the local surface stiffness of adherent cells with AFM and whole cell-body stiffness of suspended cells with optical stretcher revealed different mechanical properties (26). Therefore, to evolve the cell stiffness-based cytotechnology into a generally accepted method, it is required to characterize and compare the cell stiffness and the actin cytoskeleton structures of cancer and normal cells in both suspended and adherent states with the same experimental method.

Previously, we measured the stiffness of suspended leukocytes and trypsinized cells using AFM and a biocompatible anchor for membrane (BAM) substrate (27,28). The BAM molecule contains an oleyl group at one end that anchors the suspended cells (29). These BAM-anchored suspended cells do not move around freely like floating cells allowing us to measure their elasticity by AFM. Moreover, since BAM-anchored cells are relatively immobilized, they cannot attach to the culture substrate like adherent cells. Therefore, cell on the BAM-surface are in fact anchored suspended cells and differ from both floating and adherent cells. The morphology of substrate-adherent cells varies among cells, and the orientation and distribution of their actin cytoskeleton is anisotropic and heterogeneous. On the other hand, BAM-anchored suspended cells are round and homogeneous, and exhibit an apparent isotropic

actin cytoskeleton in the vicinity of their plasma membranes (30). These surface actin structures of the round cells show no apparent discrimination with respect to cell type. Although the surface actin of trypsinized and mitotic round cells appears to develop similarly, surface stiffness of the trypsinized round cells is greater than that of mitotic round cells (30). This surface stiffness is vanished by actin depolymerization. Thus, surface stiffness/elasticity measurement can detect invisible information about the maturation or strength of the actin cytoskeleton network near cell surface and may elucidate the difference in the regulatory mechanism of cell surface actin cytoskeleton.

In this study, we examined the surface stiffness of cancer and normal cells in the adherent and suspended states using AFM indentation method. Furthermore, the stiffness responses of the cancer and normal cells to actin cytoskeleton-modifying agents were determined in the adherent and suspended states.

Materials and Methods

Materials

The pyramidal probe (SN-AF01S-NT; spring constant: 0.02 N/m) was purchased from Seiko Instruments Inc. (Tokyo, Japan). Human fetal lung normal fibroblast TIG-1 cells (31), human cervical cancer HeLa cells, and human fibrosarcoma HT1080 cells, were obtained from Health Science Research Resources Bank (Osaka, Japan). Male Fisher 344 rats were purchased from Japan SLC (Shizuoka, Japan). Antibiotics were purchased from Sigma-Aldrich (St. Louis, MO). BAM (SUNBRIGHT OE-020CS) was purchased from NOF Corporation (Tokyo, Japan). F-actin labeling kit was purchased from AAT Bioquest, Inc. (Sunnyvale, CA). Glass based culture dishes were purchased from Asahi Glass Co., Ltd. (Tokyo, Japan). Other reagents were purchased from Sigma-Aldrich, Wako Pure Chemical Industries Ltd. (Osaka, Japan), or Life Technologies Japan Ltd. (Tokyo, Japan).

Preparation of BAM-coated dishes

BAM-coated dishes were prepared as described previously (28). Briefly, polystyrene and glass based tissue culture dishes were coated with 5% BSA in PBS for 1 h. This BSA layer prevents any non-specific cell-substrate interaction. After washing with Milli-Q water, the surfaces were treated with 1 mM BAM in PBS for 30 min. Then, the BAM-coated dishes were washed and dried.

Preparation and culture of rat MSCs

Rat MSCs were isolated and cultured as described previously (32). Briefly, bone marrow cells were obtained from the femoral shafts of 7-week-old male Fisher 344 rats. The cells were obtained from at least 2 rats and mixed. MEM containing 15% FBS and antibiotics (100 units/mL penicillin G, 100 μg/mL streptomycin sulfate, and 0.25 μg/mL amphotericin B) was used as the culture medium. The medium was renewed twice a week, and cells at passages 2–6 were used. The animal experiment was approved by the ethics committee of the National Institute of Advanced Industrial Science and Technology (AIST), Japan.

Cell culture and drug treatment

TIG-1, HeLa, and HT1080 cells were maintained in DMEM containing 10% FBS and antibiotics. The culture medium was replaced twice a week. For adherent and suspended state examination, cells were treated with Y27632 (20 μM) or calyculin A (0.1 nM) for 12 h. For the suspended state, cells were removed from the culture dish by treating with 0.25% trypsin-0.02% EDTA in PBS and plated on a BAM-coated dish for 30 min in normal culture medium, then washed with PBS to remove unattached cells, and cultured for 12 h in drug-containing medium. Viability of the cells anchored on the BAM surface indicated more than 90% after 12 h culture (data not

shown). Cells adhering to the culture dishes and BAM surfaces with or without the drug were manipulated by AFM (Fig. 1A). Actin depolymerization was induced by treating with 5 μM cytochalasin D for 2 h.

Evaluation of the actin cytoskeleton

To visualize actin cytoskeleton microstructures, cultured cells in glass based dishes with or without BAM coating were fixed with 4% paraformaldehyde, permeabilized with 0.5% Triton X-100, and stained with the F-actin labeling kit. Serial sections of specimens (0.5 μm thick) were observed by confocal laser scanning microscopy (CLSM) (FV-1000; Olympus, Tokyo, Japan) using a 60× oil immersion lens (NA = 1.42). Serial images were superimposed using ImageJ software (NIH, Bethesda, MD).

AFM measurements

Adherent and BAM-anchored suspended cells in medium were manipulated by AFM (Nanowizard I; JPK Instruments AG, Berlin, Germany) at room temperature. Combining the optical microscope (IX-71; Olympus) and AFM allows the probe to be positioned on a particular region of the cell surface. In this study, the AFM probe was indented the cell surface on the nuclear region with a force of up to 1 nN at 5 μm/s. The Young's modulus of the cell was calculated using the Hertz model (33). The force-distance curve for a region up to about 500 nm of cell surface indentation was fitted using JPK data processing software (JPK instruments AG) as

$$F = \frac{E}{1-\nu^2}\frac{\tan\alpha}{\sqrt{2}}\delta^2, \qquad (1)$$

Where F = force, δ = depth of the probe indentation, ν = Poisson's ratio (0.5), α = half-angle to the face of the pyramidal probe (20º), and E = Young's modulus (Fig. 1B). More than 20 cells were used per experiment, and 25 points were examined on the surface of each cell. The median

value was adopted as the Young's modulus of each cell (34).

Statistical analysis

The changes in the Young's modulus of cells were cluster analyzed using College Analysis software created by Prof. Masayasu Fukui (Fukuyama Heisei University, Hiroshima, Japan). We used the changes in the logarithmic average of the Young's modulus for the analysis. The responsiveness of the Young's modulus to Y27632 or calyculin A treatment in the adherent or suspended states was used as the variable in each cell. The distance of each element was calculated with the standardized Euclidean distance method and the clusters were constructed using the Ward method.

Results

Actin cytoskeleton structures of adherent and BAM-anchored suspended cancer and normal cells

In this study, we used 2 types of normal stromal cells: rat MSCs and human TIG-1 fibroblasts, and 2 cancer cell lines: HeLa and HT1080 cells. They adhered and well spread on the normal culture substrate (Supplementary Fig. S1A). After cell detachment from the culture substrate by trypsinization and anchoring onto BAM substrate, the suspended cells showed almost similar round shape irrespective of the cell type (Supplementary Fig. S1B). Upon detachment from the normal culture substrate, the morphological anisotropy of the cells was apparently canceled.

To characterize the actin cytoskeleton structures of the adherent cell types and their reorganization during the transition from the adherent to the suspended state, F-actin was stained using fluorescein-labeled phalloidin and observed by CLSM (Fig. 2). Adherent MSCs and TIG-1 cells showed highly developed actin stress fibers across the cell body and particularly bore a clear filamentous perinuclear actin cap at their apical surface. The actin cap is an F-actin structure that forms a dome above the nucleus (35). By contrast, adherent HeLa and HT1080

cells showed weak stress fibers at the basal plane and many protrusions, fillopodia, and ruffling at the edges. They did not have any developed actin cap structures but had many short microvillus structures on their surface.

On the other hand, the F-actin structures of the examined cells changed entirely on the BAM surface. Particularly similar F-actin structures were observed irrespective of the cell type so that all BAM-anchored suspended cells had clear actin structures in the vicinity of the plasma membrane (Fig. 2). Although some spotted actin structures were observed inside the cells, no filamentous structures were observed. The apical actin structures of adherent and BAM-anchored suspended cancer cells were apparently similar.

Mechanical properties of adherent and BAM-anchored suspended cancer and normal cells

We then determined the surface mechanical properties of the cells in the adherent and suspended states using the AFM indentation method. To reduce the effect of cell morphology, we placed the AFM probe on the nuclear region of the adherent cell surface. Fig. 3 shows the distribution of the Young's modulus of each cell type in the two adhesion states. The Young's modulus was broadly distributed irrespective of the cell type and cell adhesion states. Our previous studies revealed that the distribution of the Young's modulus of a cell follows a log-normal pattern (28,34). Therefore, we have shown the logarithmic average of the Young's modulus for each condition.

The distribution of the Young's moduli of adherent normal stromal cells was clearly higher than those of cancer cells (Fig. 3). Upon detachment from the substrate and alteration in actin cytoskeleton and cell morphology, the distribution of the Young's modulus of normal stromal cells decreased but that of cancer cells was relatively unchanged. Even in the suspended state, the elastic values of normal stromal cells remained higher than those of cancer cells.

The Young's moduli of adherent and BAM-anchored suspended cells were notably diminished by actin depolymerization with cytochalasin D (Supplementary Fig. S2) indicating

the significant contribution of the cell surface actin filaments to the observed mechanical properties.

Mechanical responsiveness of cancer and normal cells to perturbations of the actin cytoskeleton

To evaluate the contribution of F-actin structures to the mechanical properties, we examined the responsiveness of the mechanical properties of the cells to actin cytoskeleton-modifying agents, Y27632 and calyculin A. Y27632 is a ROCK inhibitor that prevents and attenuates stress fiber formation (36). On the other hand, calyculin A is a myosin light chain phosphatase inhibitor that activates actomyosin formation and enhances actin polymerization (37).

Addition of Y27632 to the cultured cells reduced the distribution of the Young's modulus in all the cell types and adhesion states (Fig. 4). Particularly, the Young's moduli of normal stromal cells significantly decreased both in the adherent and suspended states. On the other hand, the reduction rates of the Young's moduli of cancer cells after treatment with Y27632 were lower and almost the same in the adherent and suspended states. AfterY27632 treatment, the distribution of the Young's moduli of BAM-anchored suspended normal stromal cells became almost the same as that of BAM-anchored suspended cancer cells.

In normal stromal cells treated with calyculin A, the distributions of the Young's modulus were almost unchanged in the adherent and suspended states (Fig. 4). On the other hand, in cancer cells, the distributions of the Young's modulus were slightly increased by calyculin A treatment in both the adherent and suspended states.

Finally, we performed statistical data analysis on the mechanical responsiveness trends of the cells. The changes in the logarithmic average of the Young's modulus in response to Y27632 and calyculin A in the adherent or suspended state were used as variables in each cell type. Fig. 5A shows dendrogram of the cluster analysis in which normal stromal and cancer cells belong to distinct clusters. The responsiveness characteristics of normal stromal and cancer cells

to Y27632 and calyculin A treatment in the adherent and suspended states are shown in Fig. 5B. The square value of each responsiveness for the agents was used for this purpose. Normal stromal cells were strongly affected by only Y27632 in the adherent and suspended states. On the other hand, cancer cells were equally affected by calyculin A and Y27632. The responsiveness to actin-modifying agents was almost unchanged in the adherent and suspended states for both normal stromal and cancer cells. Therefore, the regulatory mechanisms for F-actin structures are different in normal stromal and cancer cells regardless of their adhesion states.

Discussion

This study presented an overview of the surface mechanics and actin cytoskeleton architecture of normal stromal and cancer cells in the adherent and suspended states. Adherent normal stromal cells formed highly organized actin cap and exhibited high stiffness at their apical surface, whereas adherent cancer cells lacked the actin cap and showed lower stiffness relative to the normal cells (Figs. 2,3). The actin cap is an F-actin structure that forms a dome above the nucleus, tightly regulating the shape of the nucleus in adherent fibroblasts (35). Furthermore the actin cap regulates surface stiffness and thickness of adherent rat MSCs; a developed actin cap increases surface stiffness (34). Thus, it is easily conceivable that the observed difference in the mechanical properties of adherent normal stromal and cancer cells reflects the completely different F-actin structures at the apical surface of these cell types. This finding is also consistent with the previous studies (4,17). On the other hand, detachment from the substrate and reorganization of F-actin structures into cortical actin in the vicinity of the plasma membrane, made it difficult to define a difference between actin structures of BAM-anchored suspended cancer and normal cells (Fig. 2). Nevertheless, the distribution of the Young's modulus of BAM-anchored suspended normal stromal cells remained higher than that of cancer cells (Fig. 3). We previously showed that surface stiffness of the trypsinized round cells was greater than that

of mitotic round cells, although they had similar actin structures (30). Furthermore, the elastic responsiveness of normal stromal and cancer cells to the actin-modifying agents Y27632 and calyculin A were distinct in the suspended state (Figs. 4,5). Therefore, the surface stiffness can provide the invisible information about the states and structures of the actin cytoskeleton on the cell surface. Together, these results define a key distinction between mechanical and actin cytoskeleton features of cancer and normal stromal cells.

The need for reliable biomarkers for cancer detection and analysis is critical due to complexity of the disease. Mechanical properties such as elasticity and viscosity are markers independent from the commonly used biochemical markers of cancer cells. Development of reliable methods for measuring the mechanical properties of various cell types would contribute to early cancer screening. In this study, we suggested the capability of the discrimination between cancer and normal cells in both the adherent and suspended states using cell surface stiffness. The whole-cell deformability of cancer and normal cells in the suspended state are also different, and metastatic cancer cells are easily deformed by optical stretching (3,38). Therefore, the deformability of both local-surface and whole-body of suspended cancer cells are higher than normal cells. The easy deformability of cancer cells could be due to their unique regulatory mechanisms for actin cytoskeleton, which controls the mechanical properties of cancer cells. Recently, high-speed measuring method for cell deformation throughout the narrow microchannel has been developing (39). The measuring rate has reached more than 1000 cells/s. For the future, the precise and high-speed measurement of the mechanical properties or deformability of suspended cells can be employed for cancer cytotechnology.

Acknowledgments

We thank Prof. Masayasu Fukui (Fukuyama Heisei University, Hiroshima, Japan) for permission to use his statistical analysis software, College Analysis. This work was supported by a

Grant-in-Aid for Scientific Research on Innovative Areas “Nanomedicine Molecular Science” (No. 2306) from the Ministry of Education, Culture, Sports, Science, and Technology of Japan to T.K. and J.M., and a grant for a research project on industrialization of medical innovation and technology from Okinawa Prefecture, Japan to J.M.

References

1. **Eiraku, M., Takata, N., Ishibashi, H., Kawada, M., Sakakura, E., Okuda, S., Sekiguchi, K., Adachi, T., Sasai, Y.:** Self-organizing optic-cup morphogenesis in three-dimensional culture, Nature, **472**, 51-56 (2011).

2. **Suresh, S., Spatz, J., Mills, J.P., Micoulet, A., Dao, M., Lim, C.T., Beil, M., Seufferlein, T.:** Connections between single-cell biomechanics and human disease states: gastrointestinal cancer and malaria, Acta. Biomater., **1**, 15-30 (2005).

3. **Guck, J., Schinkinger, S., Lincoln, B., Wottawah, F., Ebert, S., Romeyke, M., Lenz, D., Erickson, H.M., Ananthakrishnan, R., Mitchell, D., Kas, J., Ulvick, S., Bilby, C.:** Optical deformability as an inherent cell marker for testing malignant transformation and metastatic competence, Biophys. J., **88**, 3689-3698 (2005).

4. **Cross, S.E., Jin, Y.S., Rao, J., Gimzewski, J.K.:** Nanomechanical analysis of cells from cancer patients, Nat. Nanotechnol., **2**, 780-783 (2007).

5. **Dai, J., Sheetz, M.P.:** Mechanical properties of neuronal growth cone membranes studied by tether formation with laser optical tweezers, Biophys. J., **68**, 988-996 (1995).

6. **Trickey, W.R., Vail, T.P., Guilak, F.:** The role of the cytoskeleton in the viscoelastic properties of human articular chondrocytes, J. Orthop. Res., **22**, 131-139 (2004).

7. **Sugitate, T., Kihara, T., Liu, X.-Y., Miyake, J.:** Mechanical role of the nucleus in a cell in terms of elastic modulus, Current Applied Physics, **9**, e291-e293 (2009).

8. **Pelling, A.E., Dawson, D.W., Carreon, D.M., Christiansen, J.J., Shen, R.R., Teitell, M.A., Gimzewski, J.K.:** Distinct contributions of microtubule subtypes to cell membrane shape and stability, Nanomedicine, **3**, 43-52 (2007).

9. **Nishimura, S., Nagai, S., Katoh, M., Yamashita, H., Saeki, Y., Okada, J., Hisada, T., Nagai, R., Sugiura, S.:** Microtubules modulate the stiffness of cardiomyocytes against shear stress, Circ. Res., **98**, 81-87 (2006).

10. **Rao, J.Y., Hurst, R.E., Bales, W.D., Jones, P.L., Bass, R.A., Archer, L.T., Bell, P.B., Hemstreet, G.P., 3rd:** Cellular F-actin levels as a marker for cellular transformation: relationship to cell division and differentiation, Cancer Res., **50**, 2215-2220 (1990).
11. **Hemstreet, G.P., 3rd, Rao, J.Y., Hurst, R.E., Bonner, R.B., Jones, P.L., Vaidya, A.M., Fradet, Y., Moon, R.C., Kelloff, G.J.:** Intermediate endpoint biomarkers for chemoprevention, J. Cell Biochem. Suppl., **16I**, 93-110 (1992).
12. **Rao, J.:** Targeting actin remodeling profiles for the detection and management of urothelial cancers--a perspective for bladder cancer research, Front Biosci., **7**, e1-8 (2002).
13. **Lu, Q.Y., Jin, Y.S., Pantuck, A., Zhang, Z.F., Heber, D., Belldegrun, A., Brooks, M., Figlin, R., Rao, J.:** Green tea extract modulates actin remodeling via Rho activity in an in vitro multistep carcinogenic model, Clin. Cancer Res., **11**, 1675-1683 (2005).
14. **Evans, E., Yeung, A.:** Apparent viscosity and cortical tension of blood granulocytes determined by micropipet aspiration, Biophys. J., **56**, 151-160 (1989).
15. **Guck, J., Ananthakrishnan, R., Moon, T.J., Cunningham, C.C., Kas, J.:** Optical deformability of soft biological dielectrics, Phys. Rev. Lett., **84**, 5451-5454 (2000).
16. **Radmacher, M., Fritz, M., Kacher, C.M., Cleveland, J.P., Hansma, P.K.:** Measuring the viscoelastic properties of human platelets with the atomic force microscope, Biophys. J., **70**, 556-567 (1996).
17. **Li, Q.S., Lee, G.Y., Ong, C.N., Lim, C.T.:** AFM indentation study of breast cancer cells, Biochem. Biophys. Res. Commun., **374**, 609-613 (2008).
18. **Faria, E.C., Ma, N., Gazi, E., Gardner, P., Brown, M., Clarke, N.W., Snook, R.D.:** Measurement of elastic properties of prostate cancer cells using AFM, Analyst, **133**, 1498-1500 (2008).
19. **Fuhrmann, A., Staunton, J.R., Nandakumar, V., Banyai, N., Davies, P.C., Ros, R.:** AFM stiffness nanotomography of normal, metaplastic and dysplastic human esophageal cells,

Phys. Biol., **8**, 015007 (2011).

20. **Cross, S.E., Jin, Y.S., Lu, Q.Y., Rao, J., Gimzewski, J.K.:** Green tea extract selectively targets nanomechanics of live metastatic cancer cells, Nanotechnology, **22**, 215101 (2011).

21. **Lekka, M., Pogoda, K., Gostek, J., Klymenko, O., Prauzner-Bechcicki, S., Wiltowska-Zuber, J., Jaczewska, J., Lekki, J., Stachura, Z.:** Cancer cell recognition - Mechanical phenotype, Micron, **43**, 1259-1266 (2012).

22. **Collinsworth, A.M., Zhang, S., Kraus, W.E., Truskey, G.A.:** Apparent elastic modulus and hysteresis of skeletal muscle cells throughout differentiation, Am. J. Physiol. Cell Physiol., **283**, C1219-1227 (2002).

23. **Costa, K.D.:** Imaging and probing cell mechanical properties with the atomic force microscope, Methods Mol. Biol., **319**, 331-361 (2006).

24. **Stancel, G.A., Coffey, D., Alvarez, K., Halks-Miller, M., Lal, A., Mody, D., Koen, T., Fairley, T., Monzon, F.A.:** Identification of tissue of origin in body fluid specimens using a gene expression microarray assay, Cancer Cytopathol., **120**, 62-70 (2012).

25. **Guck, J., Ananthakrishnan, R., Mahmood, H., Moon, T.J., Cunningham, C.C., Kas, J.:** The optical stretcher: a novel laser tool to micromanipulate cells, Biophys. J., **81**, 767-784 (2001).

26. **Maloney, J.M., Nikova, D., Lautenschlager, F., Clarke, E., Langer, R., Guck, J., Van Vliet, K.J.:** Mesenchymal stem cell mechanics from the attached to the suspended state, Biophys. J., **99**, 2479-2487 (2010).

27. **Kagiwada, H., Nakamura, C., Kihara, T., Kamiishi, H., Kawano, K., Nakamura, N., Miyake, J.:** The mechanical properties of a cell, as determined by its actin cytoskeleton, are important for nanoneedle insertion into a living cell, Cytoskeleton (Hoboken), **67**, 496-503 (2010).

28. **Shimizu, Y., Kihara, T., Haghparast, S.M., Yuba, S., Miyake, J.:** Simple display system of mechanical properties of cells and their dispersion, PLoS One, **7**, e34305 (2012).
29. **Kato, K., Umezawa, K., Funeriu, D.P., Miyake, M., Miyake, J., Nagamune, T.:** Immobilized culture of nonadherent cells on an oleyl poly(ethylene glycol) ether-modified surface, Biotechniques, **35**, 1014-1021 (2003).
30. **Shimizu, Y., Haghparast, S.M., Kihara, T., Miyake, J.:** Cortical rigidity of round cells in mitotic phase and suspended state, Micron, **43**, 1246-1251 (2012).
31. **Ohashi, M., Aizawa, S., Ooka, H., Ohsawa, T., Kaji, K., Kondo, H., Kobayashi, T., Noumura, T., Matsuo, M., Mitsui, Y., Murota, S., Yamamoto, K., Ito, H., Shimada, H., Utakoji, T.:** A new human diploid cell strain, TIG-1, for the research on cellular aging, Exp. Gerontol., **15**, 121-133 (1980).
32. **Kihara, T., Hirose, M., Oshima, A., Ohgushi, H.:** Exogenous type I collagen facilitates osteogenic differentiation and acts as a substrate for mineralization of rat marrow mesenchymal stem cells in vitro, Biochem. Biophys. Res. Commun., **341**, 1029-1035 (2006).
33. **Hertz, H.:** Über die berührung fester elastischer Körper, J. reine und angewandte Mathematik, **92**, 156-171 (1881).
34. **Kihara, T., Haghparast, S.M., Shimizu, Y., Yuba, S., Miyake, J.:** Physical properties of mesenchymal stem cells are coordinated by the perinuclear actin cap, Biochem. Biophys. Res. Commun., **409**, 1-6 (2011).
35. **Khatau, S.B., Hale, C.M., Stewart-Hutchinson, P.J., Patel, M.S., Stewart, C.L., Searson, P.C., Hodzic, D., Wirtz, D.:** A perinuclear actin cap regulates nuclear shape, Proc. Natl. Acad. Sci. U S A, **106**, 19017-19022 (2009).
36. **Uehata, M., Ishizaki, T., Satoh, H., Ono, T., Kawahara, T., Morishita, T., Tamakawa, H., Yamagami, K., Inui, J., Maekawa, M., Narumiya, S.:** Calcium sensitization of smooth

muscle mediated by a Rho-associated protein kinase in hypertension, Nature, **389**, 990-994 (1997).

37. **Ishihara, H., Ozaki, H., Sato, K., Hori, M., Karaki, H., Watabe, S., Kato, Y., Fusetani, N., Hashimoto, K., Uemura, D.:** Calcium-independent activation of contractile apparatus in smooth muscle by calyculin-A, J. Pharmacol. Exp. Ther., **250**, 388-396 (1989).

38. **Lincoln, B., Erickson, H.M., Schinkinger, S., Wottawah, F., Mitchell, D., Ulvick, S., Bilby, C., Guck, J.:** Deformability-based flow cytometry, Cytometry A, **59**, 203-209 (2004).

39. **Hirose, Y., Tadakuma, K., Higashimori, M., Arai, T., Kaneko, M., Iitsuka, R., Yamanishi, Y., Arai, F.:** A new stiffness evaluation toward high speed cell sorter, Proc. 2010 IEEE Int. Conf. Robotics and Automation, 4113-4118 (2010).

Figure legends

Fig. 1 AFM manipulation of BAM-anchored suspended cells. (A) Diagram of AFM indentation of suspended cells anchored to a BAM substrate. Trypsinized, detached cells were immobilized by attaching to the BAM molecules and then indented using a pyramid-shaped AFM probe. (B) A typical force-distance curve obtained from an AFM indentation experiment on an adherent HeLa cell. The black dots represent the experimental force curve line and the grey line is the Hertz model-fitting line.

Fig. 2 CLSM images of fluorescently-labeled F-actin of cells. F-actin structures of adherent and BAM-anchored suspended cells were observed by CLSM. Superimposed images of the top, middle, and basal parts of cells are shown. The thickness of each superimposition (z) is shown in each image.

Fig. 3 Young's modulus of cells in the adherent and suspended states. The distribution and logarithmic average of the Young's moduli of the 4 cell types in adhesion (closed circles) vs. suspension states (open circles) are shown. Each condition shows the Young's modulus of 40 independent cells.

Fig. 4 Elastic responses of adherent and BAM-anchored suspended cells following treatment with Y27632 and calyculin A. The distribution and logarithmic average of the Young's moduli of the cell types in adhesion (A) and suspension (B) states are shown. Left graphs show the results of treatment with 20 μM Y27632 (Y27) and the right graphs are those of treatment with 0.1 nM calyculin A (Caly). Each condition shows the Young's modulus of 20 independent cells.

Fig. 5 Statistical analysis of the responsiveness of the Young's moduli of drug-treated adherent

and BAM-anchored suspended cells. (A) Dendrogram showing the cluster analysis of cells using the responsiveness to actin cytoskeleton-modifying agents in the adherent and suspended states. The responsiveness of the Young's modulus to Y27632 and calyculin A in the adherent or suspended states was used as variables for each cell type. (B) The elastic response behaviors of adherent and BAM-anchored suspended cells after treatment with Y27632 and calyculin A. The square values of the logarithmic average difference of the Young's modulus in the non-treated control condition from the agent-treated condition were used.

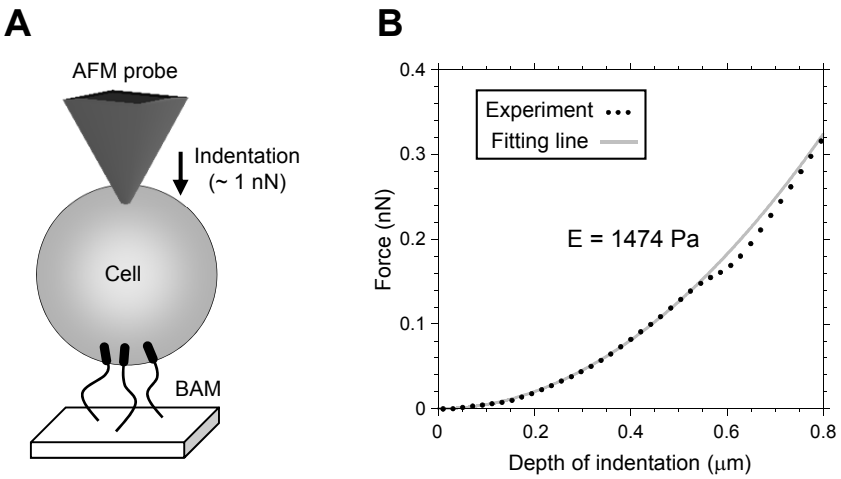

Fig. 1 Haghparast et al.

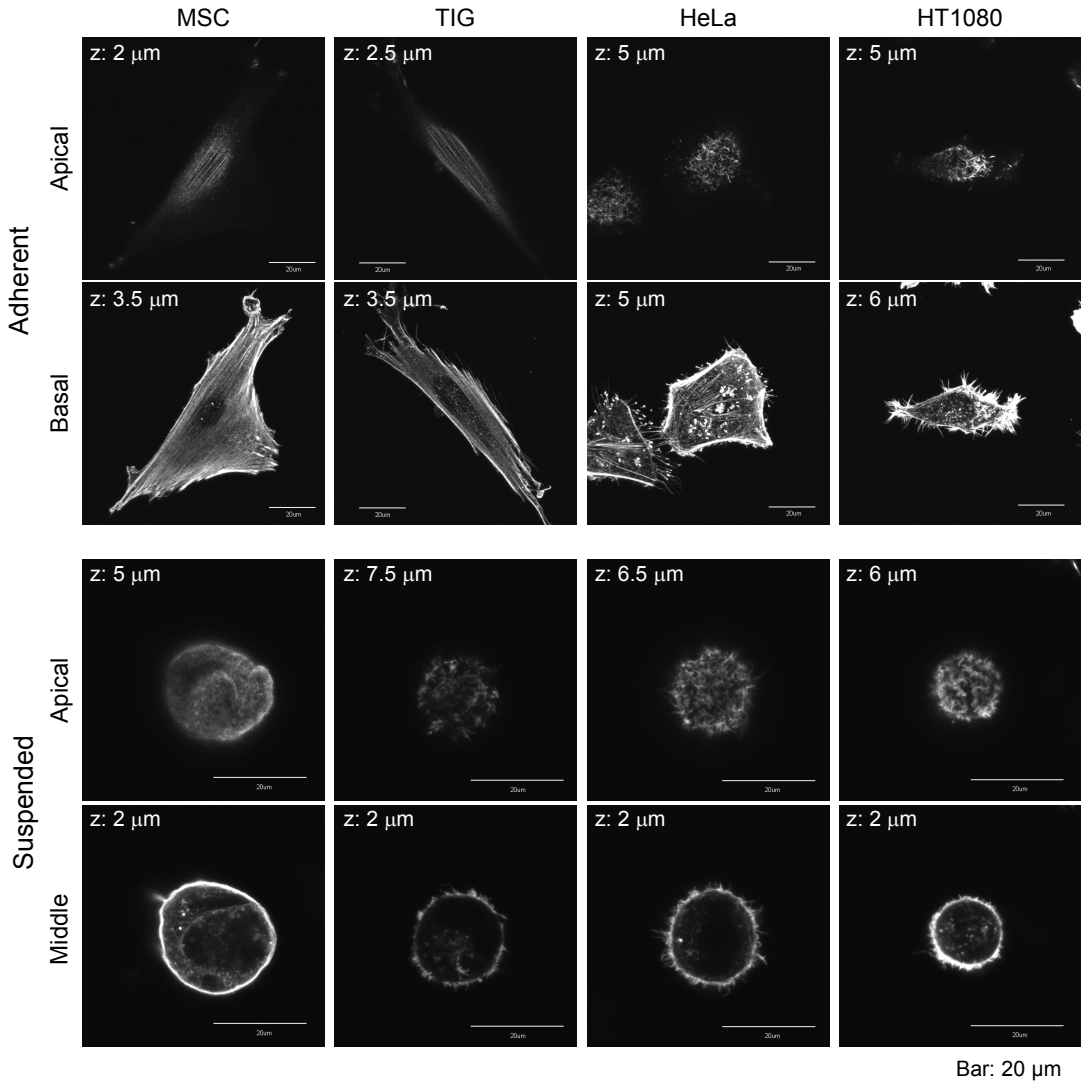

Fig. 2 Haghparast et al.

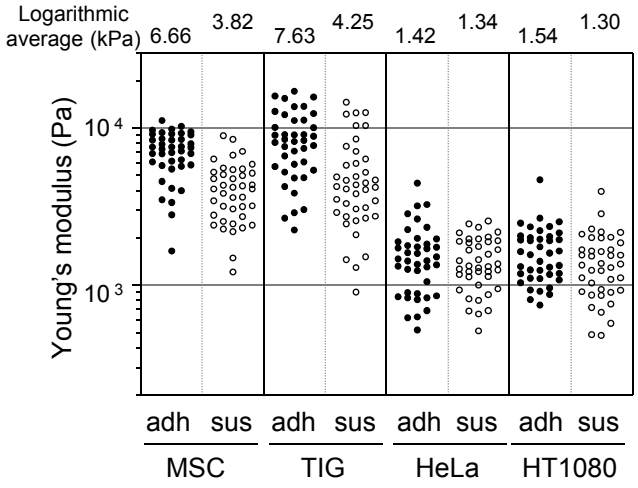

Fig. 3 Haghparast et al.

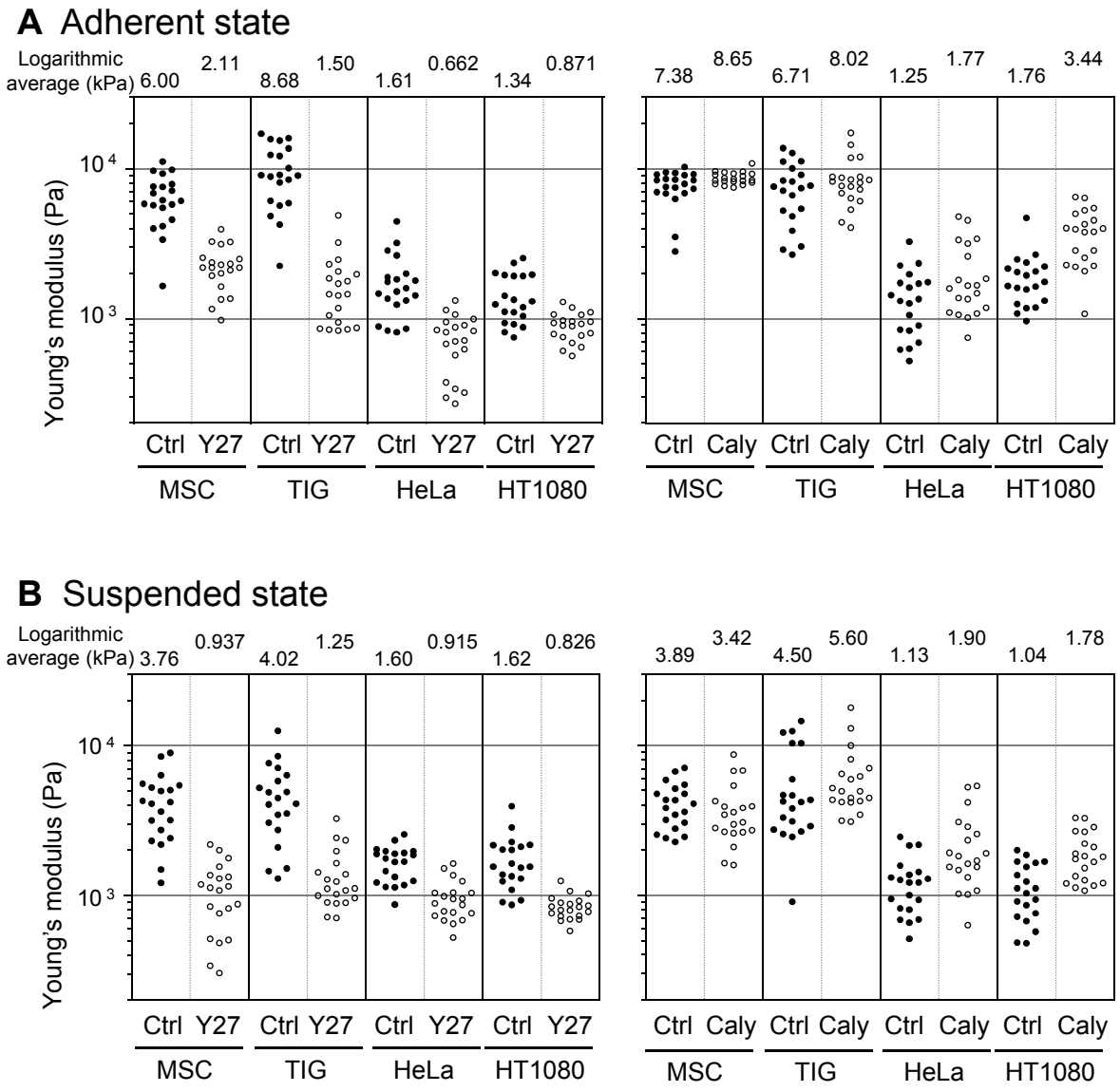

Fig. 4 Haghparast et al.

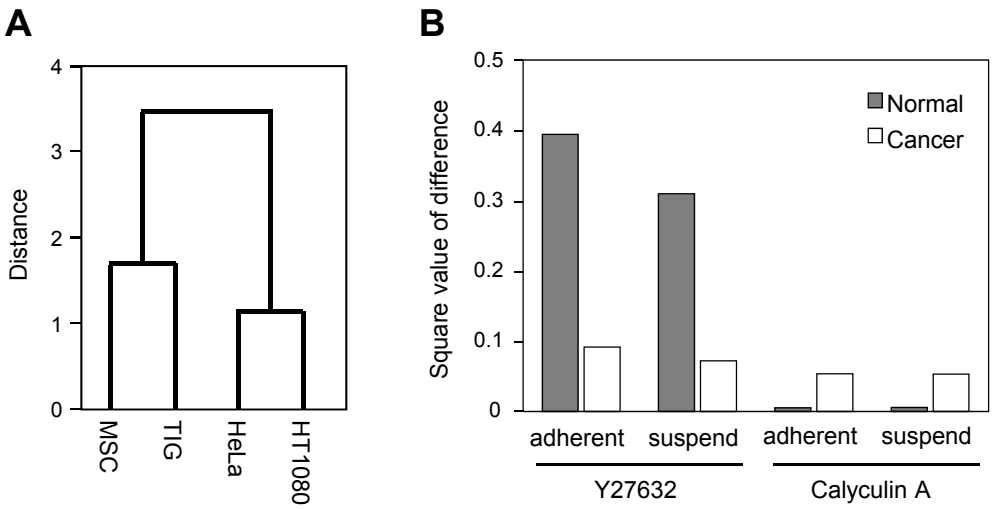

Fig. 5 Haghparast et al.

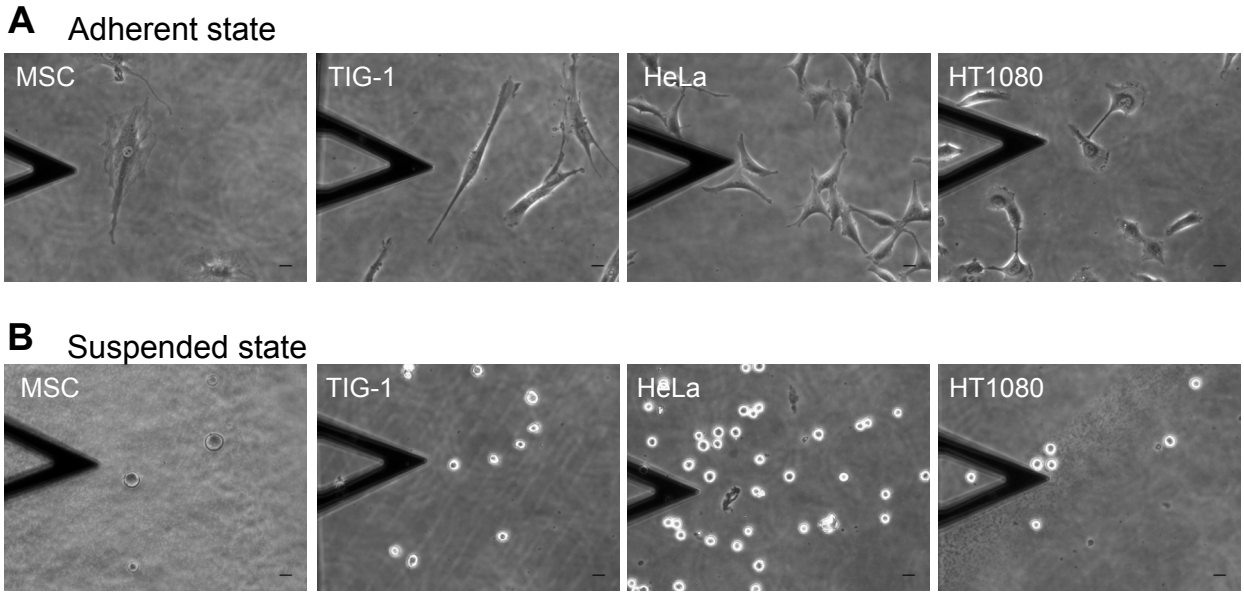

Supplementary Fig. S1 Haghparast et al.

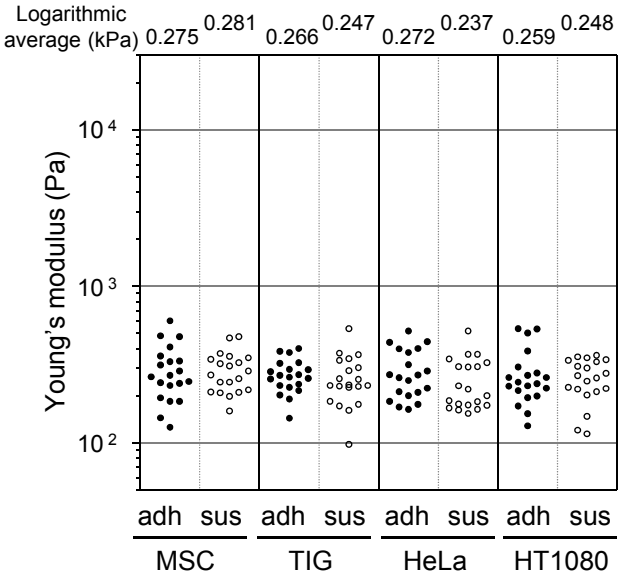

Supplementary Fig. S2 Haghparast et al.